SpinShot: Optimizing Both Physical and Perceived Force Feedback of Flywheel-Based, Directional Impact Handheld Devices

Chia-An Fan
National Taiwan University
Taipei, Taiwan
r10922109@ntu.edu.tw

En-Huei Wu
National Taiwan University
Taipei, Taiwan
r12922105@ntu.edu.tw

Chia-Yu Cheng
National Taiwan University
Taipei, Taiwan
r11922117@ntu.edu.tw

Yu-Cheng Chang
National Taiwan University
Taipei, Taiwan
r11922021@ntu.edu.tw

Alvaro Lopez
National Taiwan University
Taipei, Taiwan
r11944065@ntu.edu.tw

Yu Chen
National Taiwan University
Taipei, Taiwan
r11922026@ntu.edu.tw

Chia-Chen Chi
National Taiwan University
Taipei, Taiwan
r10921062@ntu.edu.tw

Yi-Sheng Chan
National Taiwan University
Taipei, Taiwan
b09502158@ntu.edu.tw

Ching-Yi Tsai
National Taiwan University
Taipei, Taiwan
r09944022@ntu.edu.tw

Mike Y. Chen
National Taiwan University
Taipei, Taiwan
mikechen@csie.ntu.edu.tw

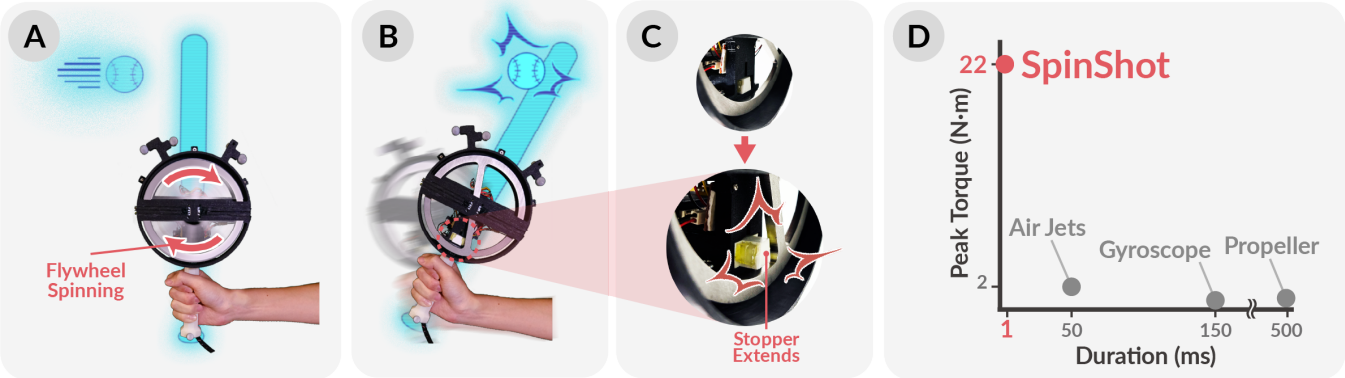

Figure 1: SpinShot introduces a flywheel-based mechanism for instantaneous impact feedback, enhancing directional impact experiences. It operates as follows: (A) The flywheel accelerates prior to impact, storing energy kinetically. (B) At the moment of impact, the device instantaneously halts the flywheel, generating torque and oscillatory forces. (C) This halt is achieved by extending a stopper to collide with the flywheel's spoke. (D) This design allows for an instantaneous impulse duration of 1 ms, offering a realistic impact experience with greater magnitude than prior directional feedback systems.

ABSTRACT

Real-world impact, such as hitting a tennis ball and a baseball, generates instantaneous, directional impact forces. However, current ungrounded force feedback technologies, such as air jets and propellers, can only generate directional impulses that are 10x-10,000x weaker. We present SpinShot, a flywheel-based device with a solenoid-actuated stopper capable of generating directional impulse of $22Nm$ in $1ms$, which is more than 10x stronger than prior ungrounded directional technologies. Furthermore, we present a novel force design that reverses the flywheel immediately after the initial impact, to significantly increase the perceived magnitude. We conducted a series of two formative, perceptual studies (n=16, 18), followed by a summative user experience study (n=16) that compared SpinShot vs. moving mass (solenoid) and vs. air jets in a VR baseball hitting game. Results showed that SpinShot significantly improved realism, immersion, magnitude ($p < .01$) compared to both baselines, but significantly reduced comfort vs. air jets primarily due to the 2.9x device weight. Overall, SpinShot was preferred by 63-75% of the participants.

UIST '24, October 13–16, 2024, Pittsburgh, PA, USA

ACM ISBN 979-8-4007-0628-8/24/10
https://doi.org/10.1145/3654777.3676433

CCS CONCEPTS

• **Human-centered computing** → **Haptic devices**.

KEYWORDS

Haptic, Impact Force, Flywheel, Handheld Device, Ungrounded Force Feedback, Perceptual Design, Virtual Reality

ACM Reference Format:
Chia-An Fan, En-Huei Wu, Chia-Yu Cheng, Yu-Cheng Chang, Alvaro Lopez, Yu Chen, Chia-Chen Chi, Yi-Sheng Chan, Ching-Yi Tsai, and Mike Y. Chen. 2024. SpinShot: Optimizing Both Physical and Perceived Force Feedback of Flywheel-Based, Directional Impact Handheld Devices. In *The 37th Annual*

ACM Symposium on User Interface Software and Technology (UIST '24), October 13–16, 2024, Pittsburgh, PA, USA. ACM, New York, NY, USA, 15 pages. https://doi.org/10.1145/3654777.3676433

1 INTRODUCTION

Real-world impact, such as hitting a tennis ball or baseball, generates instantaneous impulses with substantial force magnitude. For example, impulses for tennis [23] and baseball [3] range from 1-5ms in duration and 400-40,000N in magnitude. Extensive research has been conducted to develop and improve ungrounded force feedback technologies to allow users to move and interact freely in VR, including propellers [24, 26], air jets [51, 56], moving mass [10, 21, 54], and gyroscopic forces [8, 58].

To increase feedback magnitude, more powerful and heavier actuators can be used, such as by using larger propellers and compressed air tubing, and by using heavier moving mass and flywheels. However, device weight is a key design consideration for user comfort, mobility, and also realism in the context of the impact events being simulated— e.g., matching (or not exceeding) the weight of a tennis racket for VR tennis.

One approach to categorize target device weight is by the weights of popular real-world impact instruments:

- 100-250g: e.g., ping-pong paddles
- 250-400g: e.g., tennis rackets
- 400-900g: e.g., youth to adult baseball bats

Table 1 summarizes current directional impact feedback devices in terms of magnitude, duration, and weight, and shows that they can only achieve directional impulses of 4-40N with impulse duration from 1-500ms, which are 10x-10000x weaker than real-world tennis and baseball impact events.

This paper presents SpinShot, which explores and optimizes flywheel-based force feedback designs to:

(1) Increase the *physical* directional impulse magnitude by 10x compared to state-of-the-art systems, by significantly increasing the generated and stored momentum while maintaining a target device weight comparable to the lightest adult baseball bats.
(2) Increase the *perceived* magnitude via a novel force feedback design that takes advantage of the inherent reaction torque when accelerating flywheels, by reversing the flywheel immediately following the initial, instantaneous impact. This second, softer reaction torque is sufficiently close in time that the two impulses are perceived as a single impact event.

Our SpinShot prototype consists of a bi-directional flywheel with a solenoid-actuated stopper, as shown in Figure 1, that can generate a directional impact (1-DoF) at 22Nm in 1ms, which is more than 10x stronger than prior directional systems, as summarized in Table 1. In addition to the directional torque, it generates 220N of oscillatory force that is more than 5x larger than prior directional feedback systems.

To explore perceptual force design, we conducted a perceptual study (n=16) to evaluate: 1) *hard* stopping, 2) *soft* reaction torque, and 3) *hard + soft* combined. Results showed that the combined *hard + soft* technique is perceived to be significantly stronger vs. either technique alone ($p < .05$).

While SpinShot can generate significantly stronger directional impact feedback, flywheels have several inherent limitations, specifically: 1) reaction torque, 2) latency required for acceleration, 3) gyroscopic effects that resist changes to the flywheel's rotational axis, and 4) weight of the device. We mitigate reaction torque and latency by accelerating the flywheel as fast as possible below the users' detection threshold, which we identified through an Absolute Detection Threshold (ADT) study (n=18). To minimize the duration of gyroscopic effects, we use just-in-time acceleration prior to impact.

To evaluate the user experience of SpinShot, we developed a baseball hitting game in VR, and compared SpinShot vs. two state-of-the-art baselines: a solenoid-based moving mass device and an air jet-based device, specifically AirRacket [51]. Results from the study (n=16) showed that SpinShot significantly improved realism, immersion, and magnitude ($p < .01$) vs. both baselines. Although being much heavier than air jets (720g vs. 247g) significantly reduced comfort vs.. air jets, SpinShot was preferred overall by 63% and 75% of participants vs. moving mass and air jets, respectively.

Our key contributions are:

(1) A flywheel-based, directional impact handheld device capable of generating 10x stronger instantaneous impulse compared to prior systems.
(2) A novel perceptual force design that significantly increases the *perceived* magnitude by reversing the flywheel immediately after the initial impact.
(3) Explored mitigation techniques to address key undesirable user experiences associated with flywheels.
(4) Open-sourcing[1] of SpinShot's hardware, firmware and software so that others can experience and build upon our progress.

2 RELATED WORK

We discuss how SpinShot relates to state-of-the-art ungrounded impact feedback devices that provide: *directional* vs. *non-directional* feedback.

2.1 Directional Impact Feedback

2.1.1 Flywheels. Accelerating and decelerating flywheels generate opposing reaction torque, and such haptic feedback has been used for navigation guidance [4, 5, 55], guidance of medical procedures [14, 43], and for sword impact in VR [28]. Changing flywheel speed is achieved by altering motor speed or using external brakes. For example, DualFlywheel uses motor braking to generate 0.25Nm [55], while HapticWhirl [11] uses a drum brake to generate an impulse of approximately 1.8Nm within 300ms, which is 10x weaker and 60x slower than hitting a tennis ball (estimated to reach up to 20Nm [15] in 5ms).

To improve impact feedback, SpinShot is the first flywheel-based device with a collision-based instantaneous braking mechanism, capable of generating a torque of 22Nm in 1ms that is 10x stronger than prior flywheel handheld devices, while maintaining a weight comparable to the lightest adult baseball bats (720g vs. typically 26oz, or 737g). Additionally, we have developed a novel force design that further increases the perceived impact magnitude by augmenting

[1] Open sourced at https://github.com/ntu-hci-lab/SpinShot

Table 1: Comparison of impact feedback haptic devices (*denotes calculated values)

	Directional									Non-Directional		
Research	SpinShot	HapticWhirl [11]	MetamorphX [22]	iTorqU [57, 58]	AirRacket [51]	AirCharge [12]	Aero-plane [26]	Thor's Hammer [24]	Leviopole [44, 45]	ElasticVR [54]	Moving mass [49]	Moving mass [10]
Peak Directional Torque	22Nm	1.8Nm	0.4Nm	<1Nm	1.6Nm*	0.4Nm*	-	0.8Nm*	8.2Nm*	-	-	-
Peak Directional Force	-	-	-	-	4N	4N	7.1N	4N	27.8N	-	-	-
Peak Oscillatory Force	220N	-	-	-	-	40N	-	-	-	14N	30N	~500N
Minimum Impulse Duration	1ms	300ms	250ms	>50ms	50ms	1ms	300ms	500ms	90ms	-	-	1ms
Mechanism	Instantaneous brake	Drum brake	Gyroscopic force	Gyroscopic force	Compressed air jet	Air jet + Brake	Propeller	Propeller	Propeller x 8	Elastic band	Voice coil	Compressed air + 240g moving mass
Peak Power Consumption	240W*	360W*	23W	50.76W	-	-	208.2W	204.7W	4000W*	-	97.44W	-
Weight	720g	720g	840g	486g	107g	300g	1069g	692g	1370g	150g	340.2g	950g

the initial impulse with a secondary impulse through the immediate reversal of the stopped flywheel.

2.1.2 Air Propulsion. Key air propulsion technologies are compressed air jets [51, 56] and propellers [1, 2, 24, 26]. As summarized in Table 1, both generate a similar maximum directional force of about $4N$ in magnitude, with air jets having a faster impulse duration of $50ms$ compared to $500ms$ for propellers. Both technologies generate significant noise at $80dB$ at $4N$ [24, 26, 56], which requires the use of noise-canceling headphones. While air jet devices have significantly lighter handheld weight vs. propellers, they require being tethered to a compressed air source such as a portable air tank and compressor.

To increase the force magnitude, Leviopole [32, 44, 45] combines eight propellers to generate force in the same direction, achieving 27.8 N of thrust. However, it has considerable weight ($1370g$), length ($1430mm$), and noise ($95.3dB$). Additionally, its calculated peak power consumption is $4000W$ ($500W$ x 8), exceeding the $1800W$ ($120V$, $15A$) capacity of typical U.S. household power outlets.

AirCharge [12] has mounted air jets on rotating swingarms to accumulate momentum prior to colliding with a backstop. However, while it can generate a force up to $40N$, such force is oscillatory rather than directional, as the reciprocating dual-swingarm design creates no net angular momentum [55]. Thus, its directional force remains at $4N$, or $0.4Nm$ in torque.

In contrast, SpinShot accumulates angular momentum during the flywheel's acceleration phase, using an acceleration rate below the users' detection threshold. Upon collision, SpinShot generates an impulse with a net directional torque of $22Nm$, which is more than 10x stronger than AirRacket ($1.6Nm$) [51], AirCharge ($0.4Nm$) [12], and Thor's Hammer ($0.8Nm$) [24] while maintaining a weight similar to Thor's Hammer. It also generates an oscillatory force magnitude of $220N$ that is 5x of AirCharge [12]. Furthermore, SpinShot has significantly lower noise at $69dB$ vs. 80-93.5dB of air propulsion technologies, and does not produce strong air flows that disrupt people nearby.

2.1.3 Gyroscopic Force. Gyroscope effect-based systems can passively generate resistance during user movement [8, 20, 36]. However, to create torque impulses actively, these systems need gimbals to tilt rotating flywheels [7, 22, 38, 61].

Because device rotation not in the plane of the flywheel causes unwanted resistive feedback from gyroscopic force, strategies like dynamically adjusting the gimbal's angle [57, 58] and integrating multiple flywheels [7] are required to mitigate unwanted resistive forces. In terms of impact feedback, gyroscopic force-based devices generate slow impulses of $>50ms$ with a magnitude of $<1Nm$, which are 20x weaker than SpinShot.

2.2 Non-directional Impact Feedback

2.2.1 Linear Moving Mass. Impact feedback can be generated by physically accelerating/decelerating mass, by using solenoids [50], voice coil [21, 49], air pressure [10], and rubber bands [39, 52–54]. While oscillatory forces are generated, Newton's third law dictates that it does not produce net forces outside the device as two equal and opposite forces are generated between the moving mass and its enclosure. This results in ambiguous feedback directionality, such as only 79-93% correctly recognized feedback directions as reported by Su et al. [49]. Furthermore, unintended haptic feedback is generated when returning the moving mass to its ready position, although it can be mitigated by using slower return speeds.

In contrast, SpinShot generates net directional torque and its rotational flywheel can store significantly higher momentum to generate stronger feedback.

2.2.2 Weight-shifting. Unident [46] creates a perceived resistive force by shifting the rotational center of mass of a handheld proxy while users are swinging it. However, it can not generate impact feedback on its own. Additionally, its weight-shifting mechanism generates unintended translational forces and vibrations that are perpendicular to the feedback being simulated.

2.2.3 Electrical muscle stimulation (EMS). EMS applies electrical impulses to muscles to cause contraction. While it may cause discomfort and require the use of gel pads plus calibration per user, Impacto [34] and Paired-EMS [13] have coupled EMS with tactile stimulation to mimic forearm impact, and Farbiz et al. [18] have applied EMS to simulate impact when touching a wall and using a tennis racket. However, for EMS to simulate an external force, it must activate the muscle groups opposite to those actuated by real-life external forces. For example, while users contract biceps muscles to swing a ping-pong paddle to hit a ball in VR, EMS contracts the triceps muscles to resist the forearm movement, which is distinctly different from the haptic experience of a ball hitting the ping-pong paddle.

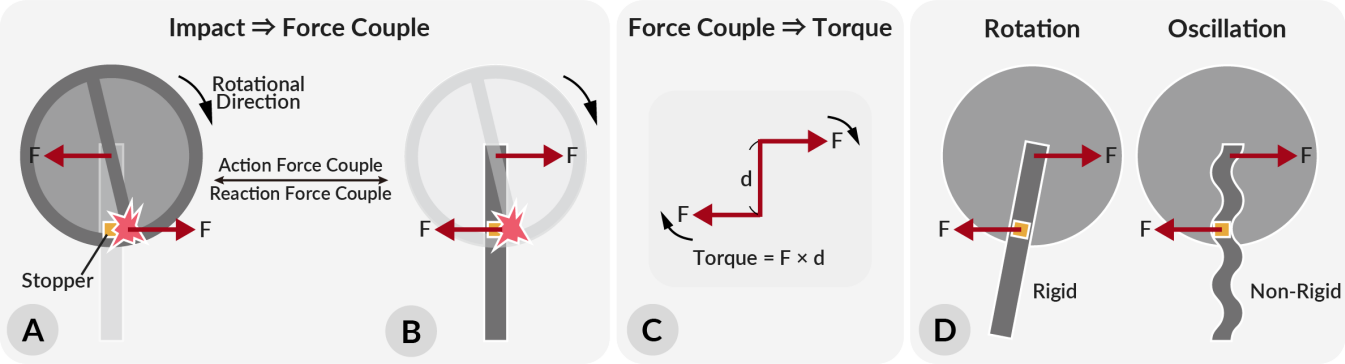

Figure 2: During impact, a pair of force couples act as action and reaction forces exerted on the flywheel and the device body: (A) One force couple stops the flywheel's rotation. (B) Another force couple applied to the device body, is capable of rotating the device. (C) This force couple acts as a torque. (D) Given the material, here are the two ideal cases when a force couple is applied to the device.

3 SYSTEM DESIGN AND IMPLEMENTATION

3.1 Design and Physics Background

SpinShot is designed to support two types of directional impulses:

(1) **Hard stopping** by stopping the flywheel using a collision-based stopper, decelerating the flywheel to $0RPM$ instantaneously in $1ms$. The magnitude of the *hard* feedback depends on the flywheel's speed at the moment of impact.
(2) **Soft reaction torque** by accelerating/decelerating the flywheel with the motor. The magnitude of this reaction torque depends on the motor's output torque, which depends on the input current, and its duration is limited by the flywheel's maximum and minimum speed.

Hard stopping generates torque through changes in angular momentum and also causes oscillation through impact. We analyzed the collision and its effects from two perspectives: the flywheel and the device body.

Flywheel Analysis: During the collision, the flywheel receives a force on its spoke from the impact point. This force acts tangentially and opposes the direction of rotation. Due to the flywheel's hub being anchored to the device, a counteracting force is applied to the flywheel through this connection, constraining it to remain attached to the device. The pair of forces, equal in magnitude and opposite in direction, and with lines of action that do not coincide, form a **force couple**, shown in Figure 2, generating torque that halts the flywheel's rotation.

Device Body Analysis: As for the device body, the reaction force couple generated from halting the flywheel is applied to it, as shown in Figure 2(B). With the torque of the couple as shown in Figure 2(C), the device applies directional haptic feedback through device rotation. If the device is rigid, only torque will be generated during the impact. However, regardless of whether the impact occurs on the device or in the real world, it results in both oscillation and torque. As a part of the impact experience, the properties of an oscillation, such as force magnitude and frequency, are affected by the materials and structure of the device. If the device is non-rigid, the force deforms the device [49], ultimately resulting in oscillation. Figure 2(D) depicts two ideal cases: one where the force couple completely translates into rotation, and the other where it entirely transforms into oscillation. In reality, the impulse results in a combination of these two effects.

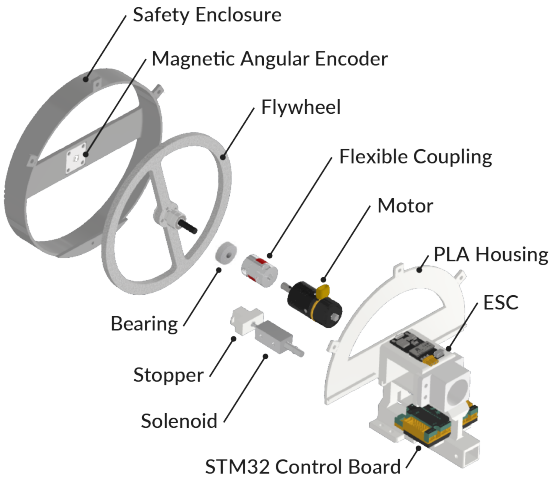

Figure 3: Exploded view of the key components of a SpinShot device (VR controller mount and optical tracking markers are not shown).

3.2 Implementation

SpinShot utilizes a motor-driven flywheel and a solenoid-actuated stopper for its feedback mechanism. To maximize SpinShot's impact magnitude while keeping the device within the target baseball bat weight class, we iterated through several designs to achieve mechanical durability. This process involved breaking multiple 3D-printed tough PLA (Polylactic Acid) housings, flywheel threading, and connectors. We also implemented flywheel tracking, motion tracking, and the integration of control circuits into a handheld haptic device. Figure 3 provides a detailed view of the key components.

3.2.1 Flywheel and Motor. We first experimented with aluminum flywheels, but found that stainless steel was needed for impact

durability. Our final design used a 6*mm* 304 stainless steel plate laser cut into a 15*cm* flywheel that weighs 278 grams, with 76% weight distributed in the rim.

For the motor, we aimed for a high torque/weight ratio, lightweight, with precision control, and a rotational speed below 1000*RPM* so the stopper has sufficient time to extend before colliding with the flywheel. We experimented with several motors and selected the RoboMaster M2006 brushless motor. It is rated at a maximum power of 240 Watts (24*V*, 10*A*), with a torque constant of 0.18*Nm/A*, and a weight of 90*g*. It is controlled via a RoboMaster C610 electronic speed controller (ESC) and has a maximum speed of approximately 550*RPM* when driving a flywheel.

We initially used a flange coupling to connect to the motor shaft using set screws, but found that the screws would slip after collision. We improved the durability by adding a bearing to support the flywheel and then connect to the motor via a flexible coupling (GFC-20x25-6x6). The flexible coupling consists of an elastic dampener in between two aluminum latches to dampen the rotational peak impact and oscillation that could damage the motor and weaken the connection to the flywheel.

To monitor the flywheel's position to actuate the stopper, we used a magnetic AS5600 encoder with a small magnet mounted on one of the spokes of the flywheel. While the motor contains an encoder, it is a relative encoder that cannot provide accurate angle information after an impact.

To support all these components and for safety, we customed 3D-printed tough PLA housing with a safety enclosure around the flywheel.

3.2.2 Stopper and Solenoid. We placed the stopper near the rim of the flywheel and close to the user's hand for the following reasons:

(1) Improved durability: a longer torque arm from the center of the flywheel reduces collision force.
(2) Reduced perceived device weight: by having a center of mass nearer to the user's hand [27].
(3) Increased perceived impact oscillation: with reduced materials between the hand and the impact location.

The stopper was 3D-printed using tough PLA, which broke after repeated collisions with the flywheel. 5*mm* polyurethane (PU) pads were placed on each side of the stopper to dampen collisions to prevent deformation or tearing. The length of the stopper was 40*mm*, and only 10*mm* would be extended beyond its housing with 30*mm* remaining inside its housing for support. The stopper is attached to the solenoid via a hot melt insert nut which provides additional dampening. The solenoid (KK-0530B) has a 10*mm* stroke with a weight of 29*g*, and has a full extension response time of 30*ms*.

3.2.3 Control System. We used the Robomaster Development Board Type C based on the STM32 microcontroller, to control all functions of the device. The board communicates with the PC via a serial port with a 500Hz sampling rate.

With the control circuit integrated, the final device measured 183 x 165 x 117*mm* (height x length x width) and weighed 720*g*, regardless of the handle weight.

3.2.4 Optical Tracking. We utilized the OptiTrack motion capture system to monitor the position and orientation of the device within the virtual environment. We attached 6 markers to the device in an arrangement that forms an asymmetrical shape. When the markers were captured by the cameras fixed in the surroundings, they would be recognized as a rigid body representing the device. The body's asymmetry enables the system to capture its orientation correctly. By aligning the coordinates of the OptiTrack system with those of the HTC Vive system, we enabled users to wield the device intuitively within the virtual space, ensuring that real-world movements are accurately mirrored in the virtual environment.

3.3 Flywheel Control

3.3.1 Acceleration State. While the current flywheel speed differs from the target speed, the system accelerates/decelerates the flywheel using a specified acceleration rate that corresponds to the current.

3.3.2 Stable State. After reaching the target speed (including 0*RPM*), the system maintains the speed of the flywheel using a proportional-integral-derivative (PID) controller. The PID controller adjusts the current supplied to the motor to maintain the flywheel at target speed, which is essential as forces from user actions, such as swinging the device, can affect the flywheel speed.

3.3.3 Impact State. To provide consistent impact collision, the stopper must be fully extended when colliding with the flywheel. Therefore, the system computes a minimum flywheel offset angle to actuate the solenoid in order to avoid partial collision.

The offset angle is calculated as follows:

$$\text{Offset Angle} \geq \text{Current Flywheel Speed} \times \text{Stopper Latency}$$

Our solenoid has a 30*ms* response time. When the flywheel speed is 550*RPM*, the offset angle would be $3.3°/ms * 30ms = 99°$. Therefore, the range of usable offset angle is 180°-99°=81° after a spoke, as monitored by the encoder.

Furthermore, to avoid motor damage due to stalling, which occurs when the motor cannot move but is still receiving power, we cut off power to the motor when a collision occurs.

4 SYSTEM EVALUATION

We evaluated the torque, oscillatory force, latency, and noise characteristics of SpinShot. All experiments were measured and averaged over 10 trials, except latency was measured for 50 trials to better understand its cumulative distribution.

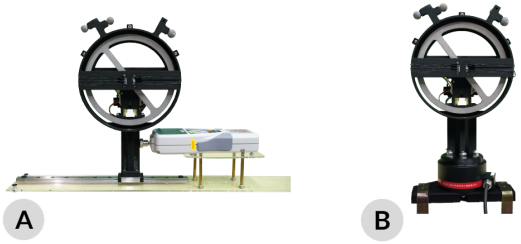

Figure 4: (A) Setup for measuring oscillatory force with an IMADA ZTS-1000N load cell. (B) Setup for measuring torque with a Decent γ74 500N-15Nm force plate.

4.1 Torque

To measure torque, we used the 6-DoF Decent γ74 500N-15Nm force plate, capable of sampling at 1000Hz with an accuracy rating of 0.3% (0.045Nm) and an overload capacity of 300% full scale (45Nm). The measurement setup is based on prior flywheel-based studies[57, 58], which bolted the device directly onto the force plate as shown in Figure 4(B).

Figure 5 shows the peak torque vs. flywheel speed, with SpinShot achieving 22.1Nm directional torque at 550RPM.

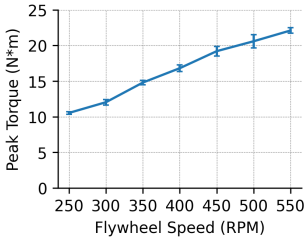

Figure 5: Peak directional torque generated by hard impact vs. flywheel speed, with error bars showing standard deviation.

4.2 Oscillatory Force

We measured oscillatory force using the IMADA ZTS-1000N load cell which has a sampling rate of 2kHz and an accuracy rating of 0.2% (2N), based on the setup used by prior impact devices [10, 12], as shown in Figure 4(A). SpinShot is placed on a moving ball-bearing platform on a gliding rail, and rests against the load cell without being attached to it.

Figure 6(A) shows the peak oscillatory force vs. flywheel speed, achieving 220N at 550RPM. Figure 6(B) shows an actual measured force-time curve that shows the initial, peak force was achieved within 1ms. It also shows device oscillation, with the device repeatedly departing from and then contacting the load cell. As a result, no negative forces were measured, and the positive forces exhibited decreasing magnitudes.

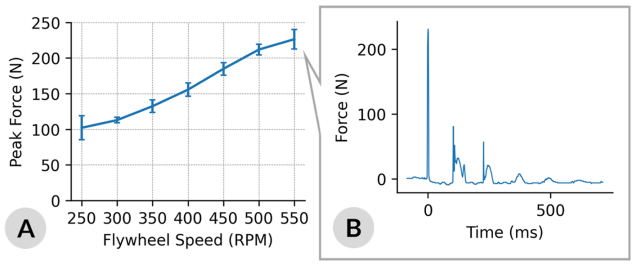

Figure 6: (A) Peak oscillatory force generated by hard impact vs. flywheel speed, with error bars showing standard deviation. (B) Illustrates an actual recorded force curve that shows device oscillation.

4.3 Flywheel Acceleration and Reaction Torque

To evaluate how fast the flywheel accelerates and the reaction torque generated, we measured the time it took to accelerate the flywheel from rest to 500RPM across different currents supplied to the motor. Additionally, we measured the reaction torque utilizing the force plate.

Figure 7 shows acceleration and peak reaction torque vs. current. With a 2A current, it took 618ms to reach 500RPM, which was an acceleration of 810RPM/s and generated reaction torque of 1.05Nm. At the maximum 10A current, the average acceleration increased to 4270RPM/s and generated a peak reaction torque of 2.85Nm.

A linear regression method was used to estimate the trends of flywheel acceleration (r^2 = 0.99) and peak reaction torque (r^2 = 0.88), facilitating an easier mapping of electric current to these two factors.

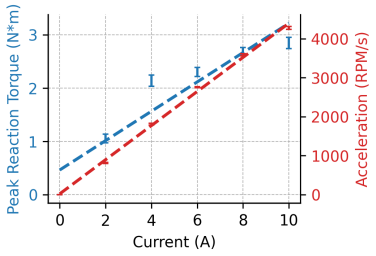

Figure 7: Average acceleration of the flywheel and reaction torque vs. current supplied to the motor, with error bars showing standard deviation, and linear regression showing the trend.

4.4 Impact Latency

When an impact is to be generated, the system has to wait until the flywheel's spokes are at angles that do not block the solenoid, before activating the stopper. Therefore, depending on the angle of the flywheel when the impact command is issued, there will be variation in the impact latency.

Device oscillation during impact makes obtaining accurate impact time only through angle tracking challenging. By summing the measured delay to reach the 20° before the collision and the estimated time required to rotate the remaining angle at each speed, we obtained the total impact latency. Figure 8 shows boxplots of the impact latency for flywheel speed of 250RPM and 550RPM, showing average latency of 91.8ms (SD=34.7) and 61.6ms (SD=16.0), respectively.

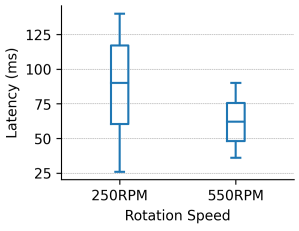

Figure 8: The impact latency from receiving the command to its actual occurrence at two rotation speeds.

4.5 Noise

To measure noise level, we used a setup based on JetController [56] and placed a WS1361C decibel meter at 1 meter distance from

the device. The experiment was conducted in an empty office surrounded by concrete walls, where the baseline ambient noise level was measured at 46dB. Figure 9 shows measured noise vs. flywheel speed. We measured the maximum system noise for the following three states: 1) maximum acceleration at 10A; 2) maximum speed of 550RPM; and 3) impact at 550RPM, all were similar at 68dB.

For reference, the Centers for Disease Control and Prevention (CDC) in the USA states that noise levels of 70dB is comparable to the noise produced by a washing machine or dishwasher, and 60dB is similar to normal conversation or the hum of an air conditioner.

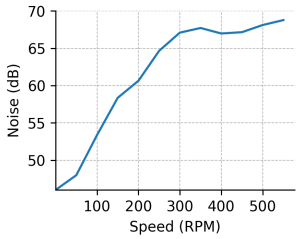

Figure 9: Measured noise level vs. flywheel speed.

5 FORCE FEEDBACK DESIGN AND PERCEPTUAL STUDY

We introduced a novel actuation design, termed *hard+soft*, by actuating *hard* and *soft* successively to increase the perceived feedback magnitude. We conducted a user study to understand the haptic experiences provided by the three types of impulses: *hard*, *soft*, and *hard+soft*.

5.1 Hard+Soft Feedback

In SpinShot, the direction of haptic feedback is determined by the direction of angular acceleration, not the rotation direction. For instance, slowing down a counter-clockwise spinning flywheel generates feedback in the same direction as accelerating a clockwise spinning flywheel, as long as the acceleration direction is the same in both cases. Based on this principle, the system first halts the flywheel through collision and then quickly reverses its direction using the motor. This process combines *hard* feedback (the strong sensation from the initial collision) with *soft* feedback (the gentler torque from the acceleration in the opposite direction) in a successive manner, all in the same direction.

5.2 Force Feedback Design

In this study, we compared three types of feedback:

(1) *Hard*: The motor speeds up the flywheel to 350RPM using a power output of 0.9A before the moment of impact. The *hard* feedback is created when the flywheel hits a stopper at this speed.
(2) *Soft*: Similarly, the motor accelerates the flywheel to 350RPM with the same power output of 0.9A. However, for *soft* feedback, the motor then quickly slows the flywheel down to 0RPM using a power output of 10A.
(3) *Hard+Soft*: Combining the previous methods, the motor first brings the flywheel up to 350RPM for a *hard* feedback event upon collision with the stopper. Then, once the flywheel comes to a stop, it is immediately spun up to 350RPM in the reverse direction with a power output of 10A to add the *soft* feedback.

Although it is possible to create *soft* feedback by either accelerating or decelerating the flywheel, we opted for generating it through deceleration. This approach ensures that the conditions before impact were consistent across all three types of feedback being compared. We selected 350RPM for the moderate force magnitude.

5.3 Participants

We recruited 16 participants, 9 male and 7 female, with ages ranging from 19 to 40 (M = 24.2, SD = 5.3), with normal or corrected-to-normal vision. All participants but one were right-handed. Four participants were familiar with VR, while the others had little to no prior experience. All participants but one had baseball-hitting experiences.

5.4 Tasks and Procedures

We used a within-subjects experimental design for pair-wise comparison of the three feedback types. Before starting the experiment, we informed the participants about the purpose of the study. To experience the impact forces generated by the device, they were asked to sit on a chair holding the device vertically with their elbow resting on the chair's armrest (the posture is shown in Figure 10). We placed VR headsets on participants, immersing them in an indoor scenario featuring a baseball pitching machine. To ensure consistent positioning of the device, we instructed participants to align it with a semi-transparent baseball bat in the VR environment and not to swing the device.

Figure 10: Study setup with a participant sitting in a chair with the dominant arm supported while holding the device.

For each pair of feedback types, participants experienced each type of feedback five times. They were asked to report the stronger feedback and rated the perceived difference in magnitude using a 5-point Likert scale, which was then combined into a 10-level strength-of-preference rating [17]. They were also asked about the qualitative differences between the two feedback conditions, the directionality of the feedback, and whether they perceived two impulses.

The three pairs of feedback types were:

- **soft** vs. *hard*
- **hard** vs. *hard+soft*
- **soft** vs. *hard+soft*

The order in which the feedback types were presented in each round was counterbalanced. However, the order of the rounds was the same for all participants, as this full counterbalancing would have required 48 participants, which was not feasible due to practical constraints. To address potential order effects [48], we carefully selected the comparison sequence. This order highlights a larger difference between *soft* and *hard* compared to *hard* and *hard+soft*. Establishing this baseline, a significant difference between *hard* and *hard+soft* would validate the experiment's findings.

5.5 Results

Figure 11 illustrates participants' ratings of perceived magnitude differences for the three comparisons using a 10-point strength-of-preference rating. In the *soft* vs. *hard* comparison, all participants reported stronger perceived magnitude for *hard*. This preference persisted in the *soft* vs. *hard+soft* comparison. In the *hard* vs. *hard+soft* comparison, 11 participants rated *hard+soft* to be stronger. While the presence of potential carryover effects might diminish the significance of the *hard* vs. *hard+soft* comparison, the two-tailed Wilcoxon one-sample signed-rank test indicated a statistically significant difference from neutral ($p < 0.05$) with a large effect size ($r > 0.5$) for all comparisons. The effect size is calculated as $r = Z/\sqrt{n}$ and interpreted using guidelines of 0.1 ~ 0.3 (small), 0.3 ~ 0.5 (moderate), and ≥ 0.5 (large) [42].

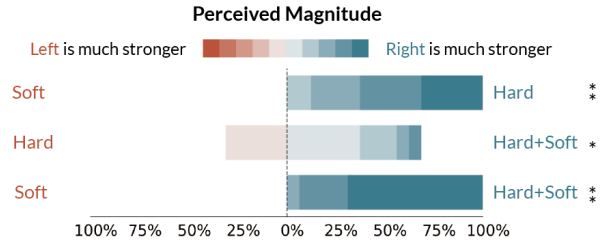

Figure 11: The ratings of perceived magnitude for the comparisons between the three feedback designs. Participants sequentially compared *soft* to *hard*, *hard* to *hard+soft*, and *soft* to *hard+soft* (significance levels: * $p < .05$, ** $p < .01$).

Apart from the difference in perceived magnitude, the participants mentioned the tactile difference in the interview. They provided similar comments when comparing *soft* vs. *hard* and *soft* vs. *hard+soft*. 10 out of 16 participants reported that the *soft* haptic feels like they are playing tee-ball (hitting with a sponge/foam bat or hitting a soft ball), and that the *hard* feedback feels like hitting a hard ball.

Regarding the comparison between *hard* and *hard+soft*, we first ensured participants treated *hard+soft* as a single event by asking if they ever felt impacted by more than one object; all answered negatively. Participants reported feeling a larger rebound with *hard+soft*: "The bat rebounds after it hits the ball" (P4/5/13), "The torque feels larger. It feels like the bat is being hit from further away from my hand, so I had to hold it tighter" (P11), and "The directionality is more net overall" (P16).

Five participants reported that *hard* had a greater magnitude than *hard+soft*, though none of them rated a large difference between the two experiences. One participant stated: "The [*hard*] feedback makes my hand feel more numb than the other one does".

All participants reported that they felt the apparent directionality of the haptic feedback. They reported: "I can feel the bat pressing against my palm" (P11), "It moved my hand/wrist/forearm" (P5/14), "I can feel that it moved in my hand" (P4/12/13/15) and "The bat tilted visually in VR" (P5/15).

6 SIDE EFFECT MITIGATION

When operating a device with a flywheel, users may experience two unintended forces: the gyroscopic effect and reaction torques. Unlike real-life scenarios, where a force is only felt upon actual impact, these effects cause users to feel incorrect forces before impact. This presents a challenge in creating a realistic experience, as we need to manage these unwanted forces that occur before the intended impact.

6.1 Gyroscopic Effect, Acceleration Latency, and Reaction Torque

When users handle a device with a rotating flywheel, they experience resistance due to the gyroscopic effect if they alter the flywheel's rotational axis. This resistance is hard to avoid and can unintentionally apply torque to the user. Despite the free movements, movements leading up to a striking action become more predictable. For example, the path of a golf club during a swing before hitting a ball is generally flat [6]. Similarly, the motion of a baseball bat before contact with the ball tends to follow a nearly straight line, with the radius of curvature averaging 1.89m ± 0.11m [25].

The gyroscopic force does not apply to the movement that is planar and parallel to the flywheel. Based on how striking motions work, we can speed up the flywheel right before impact to reduce the gyroscopic effect's influence. To achieve this rapid acceleration with minimal delay, the flywheel motor must produce more torque. However, this increased torque also causes unintended reaction torque feedback to the user. Even though SpinShot can speed up the flywheel from rest to 500 RPM in just $120ms$, it generates $2.85Nm$ of torque that acts on the user during this quick acceleration—a significant effect that cannot be overlooked.

Inspired by previous studies that revealed hand movements can impair the perception of force magnitude [60], we were intrigued by the prospect of leveraging this discovery to reduce the reaction torque.

6.2 Absolute Detection Threshold (ADT)

To explore the relationship between the sensation of reaction torque and the swing speed, we carried out an Absolute Detection Threshold (ADT) study. This research aimed to gather insights that would guide the design of actuation mechanisms to minimize unwanted reaction torque.

Participants. We recruited 18 participants (11 male, 7 female) with ages ranging from 19 to 28 ($M = 22.7$, $SD = 2.9$), and with two left-handed individuals. All participants wore noise-canceling headphones during the experiment and received nominal compensation for their participation in the study.

Procedure. The device used in the study was equipped with a handle designed for two-handed use. To examine how swing speed influences the perception of reaction torque, we divided the study into three speed categories based on our pilot study observations: slow (0.5 m/s to 1 m/s), medium (1 m/s to 3 m/s), and fast (over 3 m/s). We found that participants struggled to maintain precise speeds when swinging the device, which led us to define these speed ranges.

Participants were instructed to swing the device horizontally, ensuring that the torque experienced in the direction of the swing was caused by reaction torque, rather than by gyroscopic effects or gravity. Each trial required the participants to complete a swing spanning $80cm$. Given that most users' forearm lengths (ranging from $21.3cm$ to $25.3cm$ for East Asians [31]) determine the radius of their swing in the pilot, this effectively translates to a half-circle motion around their body.

The study applied torque toward the direction of the swing, aligned with the direction of the reaction torque before a *hard* feedback. During the swing, torque was applied only when the device was swung within these predefined speed ranges. A swing was considered valid if at least $20cm$ of its movement was within the target speed, ensuring an accurate assessment of the torque's influence. To prevent users from misinterpreting operational vibrations as reaction torque, the flywheel maintained rotation throughout the entire swing at a very low speed ($50RPM$) and power input ($0.5A$) whenever the swing speed did not meet the target range. When the swing was valid, the system then recorded the average swing speed within this target range.

Method. We used a traditional adaptive limits procedure employing a two-down, one-up staircase. The initial step was established at the maximum torque attainable by the motor (considered as $3.22Nm$ according to the regression model), with an initial step size of $0.36Nm$ ($1.1A$). After the first reversal, we halved the step size, and finished the procedure at the fifth reversal, similar to the approach used in the ADT study of HeadBlaster [33]. The ordering of the three staircases of speeds was fully counter-balanced.

Result. Figure 12 showed that ADT had a positive linear correlation to the swing speed (r=0.76). It is worth noting that all participants but one were less sensitive when they swung the device faster. 7 out of 18 participants could not perceive any additional torque even when the system applied maximum torque to them during a fast swing (>3m/s). We marked those seven users' Absolute Detection Threshold (ADT) as a step greater than the system max, as their actual ADTs were equal to or greater than this value.

6.3 ADT-based Designs

The ADT study revealed a linear relationship between the detection threshold of reaction torque and the speed of the swing. Integrating this finding with device-specific traits—that is, acceleration increased linearly with output torque, and impact magnitude increased linearly with rotation speed—led to important design considerations:

(1) With fixed feedback intensity, faster swinging allows a shorter acceleration time of the flywheel.

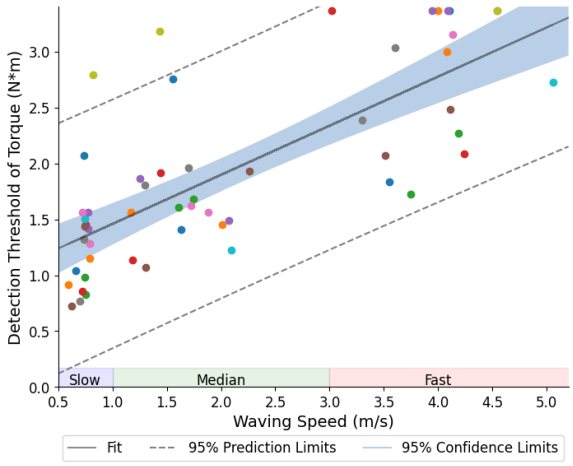

Figure 12: Linear regression shows a significant correlation between ADT of reaction torque and swing speeds (r=0.76, r^2=0.57). Colored dots represent individual user data.

(2) With fixed acceleration time, faster swinging intensifies impact feedback.

This knowledge of how various factors interplay allows game designers to customize haptic feedback based on the ADT model to fit their vision with minimum side effects. For instance, in scenarios requiring a strike, a common expectation is that faster movements produce a more substantial impact. Designers can achieve this by setting a constant acceleration time.

While the ADT study developed a model showcasing the relationship between torque detection threshold and swing speed, this model can be tailored for specific applications, particularly within VR environments. Previous research demonstrated that VR visualization can alter users' perception of feedback [9, 62]. Leveraging this insight, haptic feedback can be customized by balancing acceptable side effects with feasible acceleration speeds across various applications.

7 USER EXPERIENCE STUDY: VR BASEBALL

To evaluate SpinShot's user experience, we conducted a within-subjects study to compare its haptic feedback with two state-of-the-art baselines: a solenoid-based moving mass device and an air jet-based device, as designed in AirRacket [51]. The presentation order of the devices was fully counterbalanced both within each comparison and across different devices. We chose a baseball batting scenario for the study to focus on single, high-impact force collisions, which are common in various racket sports. This study aimed to understand user preferences in terms of immersion, realism, perceived magnitude, enjoyment, and comfort.

7.1 Baseline Devices

Two state-of-the-art devices, shown in Figure 13(B), were compared to SpinShot for user experience evaluation.

Heavy Solenoid: A Moving-Mass Approach. The moving-mass approach utilized a solenoid powered by a $240W$ supply ($24V$, $10A$),

matching SpinShot's power requirements. For a more intense experience, we chose a solenoid with a 60mm stroke length capable of producing 100N of thrust during actuation. Initially weighing 914g, we reduced the solenoid's weight to 671g by removing its unnecessary steel housing, aligning its weight more closely with that of SpinShot while maintaining its performance.

AirRacket: An Air Jet Approach. The hardware of the air-jet-based device was implemented with the open-sourced 3D models from AirRacket [51]. The weight of AirRacket measured in the paper was 258g. After replacing the handle of the original design to align with the other comparators, the weight of the AirRacket version we used was 247g. We chose the force feedback design for ping-pong proposed by AirRacket because the other two patterns (tennis and badminton) felt too soft for baseball.

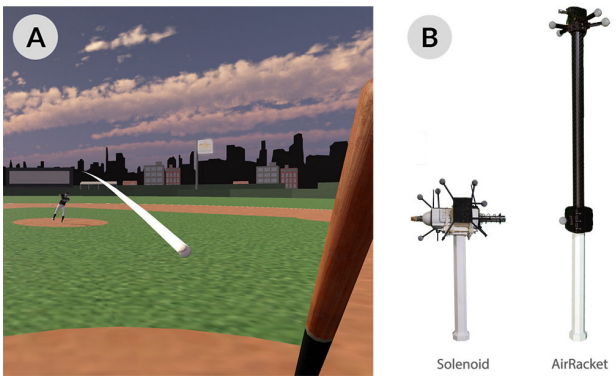

Figure 13: (A) VR baseball batting scenes used for the user evaluation. (B) The two baseline devices based on solenoids and air jets.

7.2 Feedback Design

Real-world batting delivers directional impulses significantly stronger than those produced by existing directional force technologies. While SpinShot achieved impulses 10x stronger than previous ungrounded technologies, achieving the full force of a baseball hit remained a challenge. To maximize the impact experience, the device provided feedback through the *hard+soft* actuation. The *soft* feedback in the *hard+soft* was fixed at applying maximum torque for approximately 80ms (through accelerating the flywheel reversely to 350RPM) right after the *hard* impulse.

The magnitude of *hard* feedback in the design varied. Integrating the ADT-based actuation design mentioned in Section 6, we adjusted flywheel acceleration based on pilot study insights rather than strictly following the model shown in Figure 12. Our design increased acceleration more rapidly as the swing speed increased. This design consideration accounted for the focused attention of players on visual and auditory cues in baseball games, reducing their awareness of minor unwanted feedback. This actuation strategy ensured intense feedback was applied across varying swing speeds, especially for those who swung less rapidly.

In the design, the acceleration time of the flywheel was fixed. In this situation, swinging faster enabled SpinShot to accelerate more effectively, leading to a stronger impact.

7.3 Participants

We recruited 16 participants, 8 male and 8 female, with ages ranging from 15 to 40 ($M = 22.4$, $SD = 5.4$), with normal or corrected-to-normal vision. Five participants were left-handed, and eleven were right-handed. Four participants had no prior VR experience, eight had little VR experience, and the other was familiar with VR. Seven participants had previous experience with VR haptic devices.

All participants had experience playing baseball, while four were current or retired members of a baseball team.

7.4 Tasks and Procedures

The participants stood in a safe indoor environment with enough space for them to swing the haptic devices. We asked them to participate in a VR baseball batting application (as shown in Figure 13(A)) as if they were in a real-life baseball game. In each trial, the participants would strike a ball whose speed was 72kph, and they had to complete at least 5 strikes to the outfield. Each of the comparisons was repeated twice.

Participants rated their perceived immersion, realism, magnitude, enjoyment, comfort, and overall preference using a 10-level strength-of-preference scale [17]. They were asked to compare two haptic feedback experiences and respond to the questions: "Which of the two experiences made you feel more immersed/similar to a real-world batting experience/strong in magnitude/fun/comfortable?" and to rate the significance of the differences in these attributes from 1 (neutral) to 5 (significantly different). After each response, participants were also asked to provide reasons for their choices to deepen the understanding of their preferences. The questionnaire was adapted from the original Presence Questionnaire [59], which had similarly been used in previous studies of haptic devices and VR locomotion, including AirRacket, AirCharge, Scenograph [35], and GVS-VR [47].

All participants wore noise-canceling headphones and anti-noise earmuffs during the experiment and received nominal compensation for their participation in the study.

7.5 Results

7.5.1 Baseball Batting Tasks. Across 16 participants, the averaged number of swings for SpinShot, solenoid-based, and air-jet-based devices were 36.6 ($SD = 19.1$), 14.5 ($SD = 10.9$), and 12.9 ($SD = 5.5$), respectively. The average ratio they made contact with the ball for the 3 devices was 70%, 77%, and 78%, respectively. Contact with the ball could result in outfield hits, infield hits, or foul balls.

7.5.2 Swing speed and Feedback Magnitude. For SpinShot, at the instant that the bat contacted the ball, the average swing speed was 5.59 m/s ($SD = 1.99$), and the speed of the flywheel averaged 377.7RPM ($SD = 41.6RPM$). System evaluations showed that when the *hard* impact occurs at a rotation speed ranging from 350RPM to 400RPM, the torque and oscillatory force produced are between 14.8Nm to 16.8Nm and 132N to 156N, respectively.

The average swing speed on the handle of the solenoid-based device when in contact with the ball was 6.04m/s ($SD = 3.74$). Despite variations in swing speed, the device consistently provided feedback in the form of an oscillatory force, approximately measured at 34N using the SpinShot's measurement setup.

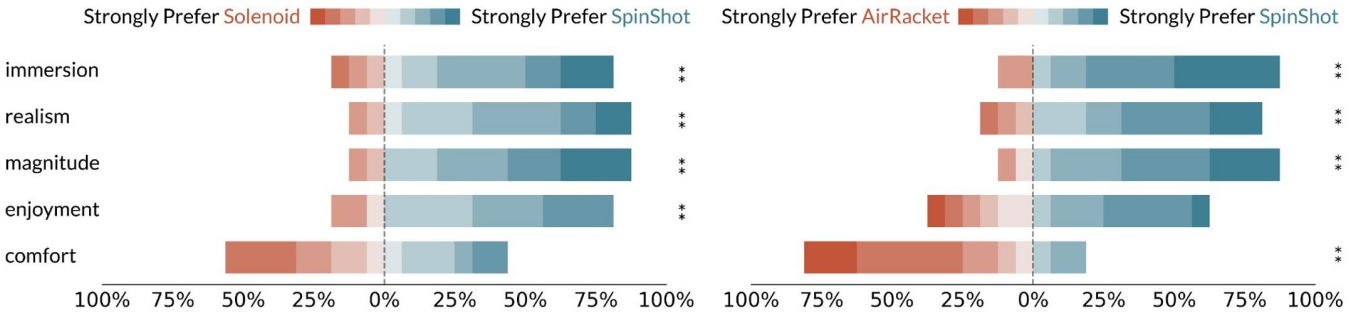

Figure 14: Immersion, realism, perceived magnitude, enjoyment and comfort of SpinShot vs. two ungrounded impact feedback baselines rated on a 10-level strength-of-preference scale: (1) moving mass (implemented with a solenoid) and (2) compressed air jet (AirRacket [51]) (significance levels: * $p < .05$, ** $p < .01$).

The average swing speed on the handle of AirRacket when in contact with the ball was 9.01m/s, faster than that of the other two approaches. Additionally, using the design of AirRacket, the feedback was related to the speed of the contact position, which is much faster than the handle speed. With the design, 99% of the swings achieved the system's maximum output of a 3.2N directional force over 114ms.

7.5.3 Ratings. Figure 14 displays the participants' ratings of perceived differences in several indicators when comparing moving mass vs. SpinShot and AirRacket vs. SpinShot.

When comparing moving mass with SpinShot, 14 out of 16 participants preferred SpinShot in terms of realism and perceived magnitude, and 13 out of 16 chose SpinShot for immersion and enjoyment. The two-tailed Wilcoxon one-sample signed-rank test showed a statistically significant difference from neutral ($p < 0.01$) with a large effect size r ≥ 0.5 for all aspects. The effect size was calculated using the formula $r = Z/\sqrt{n}$, where an r value of 0.5 or greater typically indicates a substantial effect, according to the guidelines [42]. Regarding comfort, half of the participants chose SpinShot, and the other half chose moving mass.

When comparing AirRacket with SpinShot, 14 out of 16 participants preferred SpinShot over the other in terms of perceived immersion and magnitude, and 13 out of 16 chose SpinShot for realism ($p < 0.01$, $r > 0.5$ for all). In terms of enjoyment, 10 users chose SpinShot, but there was no significance ($p = 0.07$). Regarding comfort, SpinShot was significantly worse than AirRacket ($p < 0.01$), which was disappointing but unsurprising.

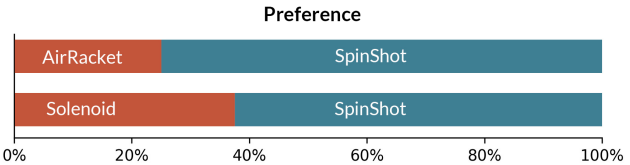

Figure 15: The overall preference of air jet and moving mass vs. SpinShot in baseball scenario.

The ratings on overall preference in both comparisons, shown in Figure 15, indicated that SpinShot was preferred by 63-75% of the participants. Although it was significantly preferred in most specific aspects, it did not show a statistical advantage over the other devices in overall preference. This implied that comfort greatly influences overall preference.

7.5.4 Qualitative Feedback. There were some similar qualitative reports from the users between the two comparisons."Its [SpinShot's] tactile feedback is more like what it will feel when hitting a baseball" (P1/4/5/7/9/10/14/15/16) and "Its [SpinShot's] magnitude on feedback is more obvious/stronger" (P2/3/5/6/8/10/11/13/14/15) were reported by many participants who preferred SpinShot in terms of immersion or realism.

Some feedback was related to the comparisons. When comparing SpinShot to moving mass, "The directionality of the haptic feedback [SpinShot] is more realistic than the other [moving mass]" (P7), and "I could only feel the feedback [of SpinShot] because the other [moving mass] was too weak to feel during swinging" (P2/6/8/13) were reported. Against AirRacket, "I can feel a recoil on the hand when I hit the ball [with SpinShot]" (P2/13) and "Its [SpinShot's] weight was more like that of a real bat [compared to AirRacket]" (P1/3/7/9/11-13/15) was mentioned. "I can only feel the feedback [of SpinShot] because the other [compressed air jet] was too weak to feel during swinging" (P2/3/6) were also reported by the participants.

Some participants also reported the advantages of the more realistic feedback. "I could realize the quality of my batting through the impact haptic" (P7) and "The feeling of SpinShot is strong enough so I could know whether I hit the ball mainly through the feeling but not visually" (P13) were reported.

7.5.5 Summary. Overall, the feedback from participants was positive, and SpinShot was preferred by 63-75% of the participants. Based on the responses, SpinShot could simulate an impact event to a high degree of strength—to enable feeling realistic haptic feedback in VR, even in the scenario requiring large magnitude feedback when swinging the handheld object. The feedback also helps participants feel more immersed in VR. Participants showed excitement with SpinShot after they tried it: "If it becomes a product, I would like to buy one" (P11) and "I just feel like I'm batting in the real world!" (P4). However, subjective responses from participants also revealed some of SpinShot's shortcomings. Participants commented that "I felt the bat is changing its shape when about to hit the ball" (P3/6), "I'm disturbed by the vibration before the impact" (P3), and "It's hard to take detailed control when swinging" (P12).

8 DISCUSSION, LIMITATIONS, FUTURE WORK

8.1 Device Vibration

One of the system's main side effects was the vibration generated during the flywheel spinning, which arose from both motor vibrations and the flywheel's wobbling. While this issue adversely affects the user experience, it can be mitigated through improved manufacturing processes, especially the flywheel's wobbling.

Imbalance, which causes the flywheel to wobble, is a common issue in high-speed rotating objects and can be reduced through the use of advanced manufacturing technologies. Specifically, dynamically balancing the wheel before it starts operating can help mitigate this problem [30]. To decrease the wobbling of SpinShot, the system not only needs to be carefully balanced but also needs a strong structure that can maintain the balance after collisions.

8.2 Size vs. Kinetic Energy

The torque the device can generate is proportional to the flywheel's moment of inertia and its angular acceleration. By implementing a collision-based mechanism that reduces the braking time to less than $1ms$ [10, 12], the maximum feedback magnitude that SpinShot can achieve is determined by the moment of inertia of the flywheel and its maximum rotation speed.

When a flywheel is well-designed so its weight is concentrated at the rim, the moment of inertia depends on two key factors:

- The weight of the flywheel
- The square of its diameter

While a larger moment of inertia in the flywheel allows the device to produce feedback across a broader range, the resulting increase in the device's size can make it impractical for some haptic applications.

Increasing the flywheel's maximum speed is more beneficial than increasing its size—from the perspective of optimizing the flywheel alone. The limit to how fast the flywheel can spin is determined by the specific motor and stopper mechanism used in the design. A more powerful motor typically increases in size, leading to a bulkier overall design. A design with faster flywheel speed also needs a stopper with a faster extension speed, because the collision-base design requires the stopper to be fully extended within a certain wheel rotation angle.

Overall, broadening the system's range of feedback magnitude usually comes with a larger device size. However, the required feedback intensity can differ significantly between various applications, necessitating a balance between device size and feedback capability.

8.3 Limitations of the ADT-based Designs

The ADT-based actuation design, detailed in Section 6, addresses the issue of unwanted reaction torque and gyroscopic force. By accelerating the flywheel to speeds just below what users can perceive, this design minimizes the impact of these forces. This method stands out from traditional approaches that rely on a low, steady output for controlling reaction torque. It offers faster response times and reduces the chance of the gyroscopic effect altering the user experience. However, in certain scenarios, its performance may be comparable to previous designs:

(1) Situations requiring high-frequency feedback while the device remains stationary in the user's hands, such as using a machine gun in a shooting game.
(2) Actions that involve rotating the device suddenly at the end, like executing a cut shot in table tennis.

To address hard actuation's limitations, applications can blend in *soft* feedback. Despite *soft* actuation's lower torque (max $2.85Nm$) and gentler sensation, it bypasses pre-impact reaction torque and gyroscopic issues, offering immediate feedback upon flywheel activation. For instance, in Half-Life Alyx, a highly-rated best-selling VR game, *hard* actuation can deliver impactful low-frequency feedback (e.g., using an axe or shotgun), while *soft* actuation is suited for high-frequency sensations (e.g., submachine gun at $10Hz$).

8.4 Impact Latency

SpinShot has an actuation-to-impact latency ranging from $61.6ms$ to $91.8ms$, depending on the speed of the flywheel, which is slightly longer than the $50ms$ threshold for visual-tactile synchronicity [16]. While no users reported perceived latency from our VR baseball user experience study, this latency can be masked by using motion prediction techniques, such as continuous hand trajectory prediction [19], which demonstrated a Root Mean Square Error (RMSE) of $0.85cm$ for predicting future hand positions up to $200ms$ ahead.

While these motion prediction techniques can mask impact latency, they were not utilized in the baseball game used for the summative application study. Despite this, users significantly preferred SpinShot in terms of realism, immersion, and perceived magnitude compared to the other mechanisms tested.

8.5 Multi-DoF Extension

SpinShot's current design supports 1-DoF, bi-directional feedback, which is suitable for simulating experiences such as sword clashes, racket sports, fishing, and the recoil forces of firing weapons. For scenarios that require feedback in more than 1-DoF, iTorqU's [58] gimbal-based approach that rotates the 1-DoF actuator can be added, although with the tradeoff of increasing device size, weight, and the possibility of unintended gyroscopic forces.

8.6 Device Durability

During and after an impact, the device absorbs some of the energy and transfers the remaining energy to the users. The amount that the device flexes–its deformability—is influenced by factors such as its material [40], its structural characteristics like thickness [29], and environmental conditions like temperature [41]. If the force from the impact exceeds the device's resilience, the device would have sustained damages.

Figure 16 shows examples of failed prototypes. Damage often manifests at a prototype's weakest spot, yet this does not indicate that the damaged part is the sole component unable to withstand the impulse. During the prototyping process, we broke over twenty 3D-printed parts, three kinds of motor-to-flywheel couplings, more than five flange connectors and shafts, and three solenoids. While our current prototype has already sustained more than 1000 impacts during the process of system evaluation, haptic design, and user studies, we have not conducted a formal durability evaluation, such as by using the test designs introduced by Kurt Munson et al. [37].

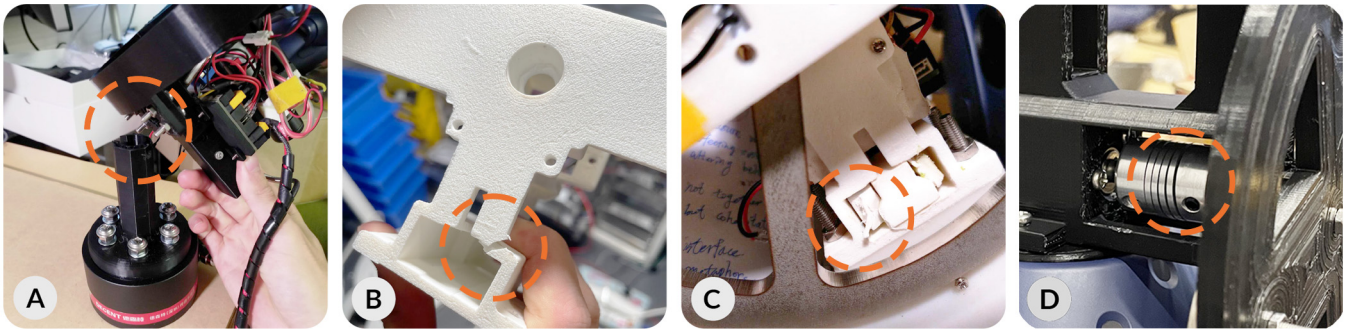

Figure 16: Examples of failed prototypes: (A) broken 3D-printed handle due to the torque and shock of the flywheels; (B) cracked 3D-printed housing around the solenoid stopper; (C) worn rubber dampener for the stopper. (D) irreversibly deformed aluminum flexible coupling, which eventually fractured after several uses due to increasing deformation.

9 CONCLUSION

We presented SpinShot, a flywheel-based force feedback device designed to deliver instantaneous impact forces by optimizing the physical feedback design and by introducing a novel perceptual feedback design. By utilizing a solenoid-actuated stopper to halt the flywheel, SpinShot generates a directional impulse of $22Nm$ in $1ms$—achieving force magnitudes 10x greater than existing ungrounded directional feedback devices while maintaining its weight at $720g$. Our novel force design, which reverses the flywheel right after the initial impact, significantly enhances the perceived magnitude of the feedback. Comparative user studies within a VR baseball simulation demonstrated that SpinShot notably improved realism, immersion, and perceived force magnitude, and was overall preferred by most participants vs. moving mass (solenoid) and air jet methods. Furthermore, our comprehensive analysis of the underlying physics and design principles of this instantaneous directional impact system provides insights for haptic developers. To foster further research and development in this area, we have open-sourced SpinShot's hardware and software.

ACKNOWLEDGMENTS

This work is supported by National Science and Technology Council and Ministry of Education, Taiwan (NSTC 112-2221-E-002-185; MOE 113L900902) and National Taiwan University. We thank Lung-pang Cheng for his invaluable feedback and support with the optical tracking system, and Ruo-pu Wang for his assistance. We also thank all participants and reviewers for their feedback.

REFERENCES

[1] Muhammad Abdullah, Minji Kim, Waseem Hassan, Yoshihiro Kuroda, and Seokhee Jeon. 2018. HapticDrone: An encountered-type kinesthetic haptic interface with controllable force feedback: Example of stiffness and weight rendering. In *2018 IEEE Haptics Symposium (HAPTICS)*. IEEE, Piscataway, NJ, USA, 334–339. https://doi.org/10.1109/HAPTICS.2018.8357197

[2] Parastoo Abtahi, Benoit Landry, Jackie (Junrui) Yang, Marco Pavone, Sean Follmer, and James A. Landay. 2019. Beyond The Force: Using Quadcopters to Appropriate Objects and the Environment for Haptics in Virtual Reality. In *Proceedings of the 2019 CHI Conference on Human Factors in Computing Systems* (Glasgow, Scotland Uk) *(CHI '19)*. Association for Computing Machinery, New York, NY, USA, 1–13. https://doi.org/10.1145/3290605.3300589

[3] Robert K Adair. 1995. The physics of baseball. *Physics Today* 48, 5 (1995), 26–31.

[4] Tomohiro Amemiya and Hiroaki Gomi. 2013. Directional Torque Perception with Brief, Asymmetric Net Rotation of a Flywheel. *IEEE Transactions on Haptics* 6, 3 (2013), 370–375. https://doi.org/10.1109/TOH.2012.38

[5] Hideyuki Ando, Kazutoshi Obana, Maeda Sugimoto, and Taro Maeda. 2002. A wearable force display based on brake change in angular momentum. *Proc. 12th Int. Conf. on Artificial Reality and Telexistence, Tokyo, 2002* null, null (12 2002), 16–21.

[6] Denise McGrath Andrew Morrison and Eric S. Wallace. 2018. The relationship between the golf swing plane and ball impact characteristics using trajectory ellipse fitting. *Journal of Sports Sciences* 36, 3 (2018), 303–310. https://doi.org/10.1080/02640414.2017.1303187 arXiv:https://doi.org/10.1080/02640414.2017.1303187 PMID: 28294698.

[7] Michele Antolini, Monica Bordegoni, and Umberto Cugini. 2011. A haptic direction indicator using the gyro effect. In *2011 IEEE World Haptics Conference*. IEEE, Istanbul, Turkey, 251–256. https://doi.org/10.1109/WHC.2011.5945494

[8] Akash Badshah, Sidhant Gupta, Daniel Morris, Shwetak Patel, and Desney Tan. 2012. GyroTab: A Handheld Device That Provides Reactive Torque Feedback. In *Proceedings of the SIGCHI Conference on Human Factors in Computing Systems* (Austin, Texas, USA) *(CHI '12)*. Association for Computing Machinery, New York, NY, USA, 3153–3156. https://doi.org/10.1145/2207676.2208731

[9] Yuki Ban and Yusuke Ujitoko. 2021. Hit-Stop in VR: Combination of Pseudo-haptics and Vibration Enhances Impact Sensation. In *2021 IEEE World Haptics Conference (WHC)*. IEEE, Montreal, QC, Canada, 991–996. https://doi.org/10.1109/WHC49131.2021.9517129

[10] Jose Luis Berna-Moya and Diego Martinez-Plasencia. 2019. Exploring the effects of replicating shape, weight and recoil effects on VR shooting controllers. In *Human-Computer Interaction–INTERACT 2019: 17th IFIP TC 13 International Conference, Paphos, Cyprus, September 2–6, 2019, Proceedings, Part I 17*. Springer, Springer, Cham, Switzerland, 763–782.

[11] Jose Luis Berna Moya, Anke van Oosterhout, Mark T Marshall, and Diego Martinez Plasencia. 2024. HapticWhirl, a Flywheel-Gimbal Handheld Haptic Controller for Exploring Multimodal Haptic Feedback. *Sensors* 24, 3 (2024), 935.

[12] Po-Yu Chen, Ching-Yi Tsai, Wei-Hsin Wang, Chao-Jung Lai, Chia-An Fan, Shih Chin Lin, Chia-Chen Chi, and Mike Y. Chen. 2023. AirCharge: Amplifying Ungrounded Impact Force by Accumulating Air Propulsion Momentum. In *Proceedings of the 36th Annual ACM Symposium on User Interface Software and Technology* (San Francisco, CA, USA) *(UIST '23)*. Association for Computing Machinery, New York, NY, USA, Article 7, 11 pages. https://doi.org/10.1145/3586183.3606768

[13] Chia-Yu Cheng, Yu Chen, Sitaresmi Wahyu Handani, Avijit Balabantaray, and Mike Y. Chen. 2024. Paired-EMS: Enhancing Electrical Muscle Stimulation (EMS)-based Force Feedback Experience by Stimulating Both Muscles in Antagonistic Pairs. In *Proceedings of the CHI Conference on Human Factors in Computing Systems* (Honolulu, HI, USA) *(CHI '24)*. Association for Computing Machinery, New York, NY, USA, Article 426, 7 pages. https://doi.org/10.1145/3613904.3642841

[14] Wenqiang Chi, Hedyeh Rafii-Tari, Christopher J. Payne, Jindong Liu, Celia Riga, Colin Bicknell, and Guang-Zhong Yang. 2017. A learning based training and skill assessment platform with haptic guidance for endovascular catheterization. In *2017 IEEE International Conference on Robotics and Automation (ICRA)*. IEEE, Singapore, 2357–2363. https://doi.org/10.1109/ICRA.2017.7989273

[15] Rod Cross. 2010. Impact forces and torques transmitted to the hand by tennis racquets. *Sports Technology* 3, 2 (2010), 102–111.

[16] Massimiliano Di Luca and Arash Mahnan. 2019. Perceptual Limits of Visual-Haptic Simultaneity in Virtual Reality Interactions. In *2019 IEEE World Haptics Conference (WHC)*. IEEE, Tokyo, Japan, 67–72. https://doi.org/10.1109/WHC.2019.8816173

[17] Ioannis Evangelidis. 2023. Task sensitivity and noise: How mechanical properties of preference elicitation tasks account for differences in preferences across tasks. *Decision* 11, 2 (May 2023), 283–302. https://doi.org/10.1037/dec0000218

[18] Farzam Farbiz, Zhou Hao Yu, Corey Manders, and Waqas Ahmad. 2007. An Electrical Muscle Stimulation Haptic Feedback for Mixed Reality Tennis Game. In *ACM SIGGRAPH 2007 Posters* (San Diego, California) *(SIGGRAPH '07)*. Association for Computing Machinery, New York, NY, USA, 140–es. https://doi.org/10.1145/1280720.1280873

[19] Nisal Menuka Gamage, Deepana Ishtaweera, Martin Weigel, and Anusha Withana. 2021. So Predictable! Continuous 3D Hand Trajectory Prediction in Virtual Reality. In *The 34th Annual ACM Symposium on User Interface Software and Technology* (Virtual Event, USA) *(UIST '21)*. Association for Computing Machinery, New York, NY, USA, 332–343. https://doi.org/10.1145/3472749.3474753

[20] Jan Gugenheimer, Dennis Wolf, Eythor R. Eiriksson, Pattie Maes, and Enrico Rukzio. 2016. GyroVR: Simulating Inertia in Virtual Reality using Head Worn Flywheels. In *Proceedings of the 29th Annual Symposium on User Interface Software and Technology* (Tokyo, Japan) *(UIST '16)*. Association for Computing Machinery, New York, NY, USA, 227–232. https://doi.org/10.1145/2984511.2984535

[21] Titan Haptics. 2023. TacHammer. https://www.titanhaptics.com/tachammer

[22] Takeru Hashimoto, Shigeo Yoshida, and Takuji Narumi. 2022. MetamorphX: An Ungrounded 3-DoF Moment Display That Changes Its Physical Properties through Rotational Impedance Control. In *Proceedings of the 35th Annual ACM Symposium on User Interface Software and Technology* (Bend, OR, USA) *(UIST '22)*. Association for Computing Machinery, New York, NY, USA, Article 72, 14 pages. https://doi.org/10.1145/3526113.3545650

[23] H Hatze. 1976. Forces and duration of impact, and grip tightness during the tennis stroke. *Med. Sci. Sports* 8, 2 (1976), 88–95.

[24] Seongkook Heo, Christina Chung, Geehyuk Lee, and Daniel Wigdor. 2018. Thor's Hammer: An Ungrounded Force Feedback Device Utilizing Propeller-Induced Propulsive Force. In *Proceedings of the 2018 CHI Conference on Human Factors in Computing Systems* (Montreal QC, Canada) *(CHI '18)*. Association for Computing Machinery, New York, NY, USA, 1–11. https://doi.org/10.1145/3173574.3174099

[25] Gen Horiuchi and Shinji Sakurai. 2016. Kinetic analyses on increase of bat head speed in baseball batting. *International Journal of Sport and Health Science* 14 (2016), 94–101.

[26] Seungwoo Je, Myung Jin Kim, Woojin Lee, Byungjoo Lee, Xing-Dong Yang, Pedro Lopes, and Andrea Bianchi. 2019. Aero-Plane: A Handheld Force-Feedback Device That Renders Weight Motion Illusion on a Virtual 2D Plane. In *Proceedings of the 32nd Annual ACM Symposium on User Interface Software and Technology* (New Orleans, LA, USA) *(UIST '19)*. Association for Computing Machinery, New York, NY, USA, 763–775. https://doi.org/10.1145/3332165.3347926

[27] Idsart Kingma, Rolf Van De Langenberg, and Peter J Beek. 2004. Which mechanical invariants are associated with the perception of length and heaviness of a nonvisible handheld rod? Testing the inertia tensor hypothesis. *Journal of Experimental Psychology: Human Perception and Performance* 30, 2 (2004), 346.

[28] Daijiro Koga and Takahiro Itagaki. 2002. Virtual Chanbara. In *ACM SIGGRAPH 2002 Conference Abstracts and Applications* (San Antonio, Texas) *(SIGGRAPH '02)*. Association for Computing Machinery, New York, NY, USA, 83. https://doi.org/10.1145/1242073.1242118

[29] A Kotousov, Paolo Lazzarin, Filippo Berto, and S Harding. 2010. Effect of the thickness on elastic deformation and quasi-brittle fracture of plate components. *Engineering Fracture Mechanics* 77, 11 (2010), 1665–1681.

[30] Rainer Leuschke. 2004. *Motor integrated actuation for a flywheel energy storage system.* University of Washington, Seattle, WA, USA.

[31] Yu-Cheng Lin, Mao-Jiun J. Wang, and Eric M. Wang. 2004. The comparisons of anthropometric characteristics among four peoples in East Asia. *Applied Ergonomics* 35, 2 (2004), 173–178. https://doi.org/10.1016/j.apergo.2004.01.004

[32] Kao-Hua Liu, Tomoya Sasaki, Hiroyuki Kajihara, Atsushi Hiyama, Masahiko Inami, and Chien-Hsu Chen. 2020. Virtual kayaking: a local culture-based virtual reality paddling experience. In *Human Aspects of IT for the Aged Population. Healthy and Active Aging: 6th International Conference, ITAP 2020, Held as Part of the 22nd HCI International Conference, HCII 2020, Copenhagen, Denmark, July 19–24, 2020, Proceedings, Part II 22*. Springer, Springer, Cham, Switzerland, 630–642.

[33] Shi-Hong Liu, Pai-Chien Yen, Yi-Hsuan Mao, Yu-Hsin Lin, Erick Chandra, and Mike Y. Chen. 2020. HeadBlaster: A Wearable Approach to Simulating Motion Perception Using Head-Mounted Air Propulsion Jets. *ACM Trans. Graph.* 39, 4, Article 84 (aug 2020), 12 pages. https://doi.org/10.1145/3386569.3392482

[34] Pedro Lopes, Alexandra Ion, and Patrick Baudisch. 2015. Impacto: Simulating Physical Impact by Combining Tactile Stimulation with Electrical Muscle Stimulation. In *Proceedings of the 28th Annual ACM Symposium on User Interface Software & Technology* (Charlotte, NC, USA) *(UIST '15)*. Association for Computing Machinery, New York, NY, USA, 11–19. https://doi.org/10.1145/2807442.2807443

[35] Sebastian Marwecki and Patrick Baudisch. 2018. Scenograph: Fitting Real-Walking VR Experiences into Various Tracking Volumes. In *Proceedings of the 31st Annual ACM Symposium on User Interface Software and Technology* (Berlin, Germany) *(UIST '18)*. Association for Computing Machinery, New York, NY, USA, 511–520. https://doi.org/10.1145/3242587.3242648

[36] Hirokazu Miyahara, Yasutoshi Makino, and Hiroyuki Shinoda. 2018. Inducing Wrist Twist During Arm Swing by Using Gyro Effect. In *Haptic Interaction: Science, Engineering and Design 2*. Springer, Springer, Berlin, Heidelberg, 205–209.

[37] Kurt Munson, Umur Yenal, and Peter Lavelle. 2018. *Durability test design: linking fatigue and reliability.* Technical Report. SAE Technical Paper.

[38] Martin Murer, Bernhard Maurer, Hermann Huber, Ilhan Aslan, and Manfred Tscheligi. 2015. TorqueScreen: Actuated Flywheels for Ungrounded Kinaesthetic Feedback in Handheld Devices. In *Proceedings of the Ninth International Conference on Tangible, Embedded, and Embodied Interaction* (Stanford, California, USA) *(TEI '15)*. Association for Computing Machinery, New York, NY, USA, 161–164. https://doi.org/10.1145/2677199.2680579

[39] Juan F. Olaya-Figueroa, Ferdinand Streicher, Marco Kurzweg, Jan Willms, and Katrin Wolf. 2023. HapticCollider: Ungrounded Force Feedback for Rigid Collisions during Virtual Tool Use. In *Proceedings of Mensch Und Computer 2023* (Rapperswil, Switzerland) *(MuC '23)*. Association for Computing Machinery, New York, NY, USA, 116–126. https://doi.org/10.1145/3603555.3603568

[40] Dongxue Qin, Lin Sang, Zihui Zhang, Shengyuan Lai, and Yiping Zhao. 2022. Compression performance and deformation behavior of 3D-printed PLA-based lattice structures. *Polymers* 14, 5 (2022), 1062.

[41] F. Rezgui, M. Swistek, J.M. Hiver, C. G'Sell, and T. Sadoun. 2005. Deformation and damage upon stretching of degradable polymers (PLA and PCL). *Polymer* 46, 18 (2005), 7370–7385. https://doi.org/10.1016/j.polymer.2005.03.116 Stimuli Responsive Polymers.

[42] Robert Rosenthal, Harris Cooper, Larry Hedges, et al. 1994. Parametric measures of effect size. *The handbook of research synthesis* 621, 2 (1994), 231–244.

[43] Evren Samur, Lionel Flaction, Ulrich Spaelter, Hannes Bleuler, David Hellier, and Sebastien Ourselin. 2008. A Haptic Interface with Motor/Brake System for Colonoscopy Simulation. In *2008 Symposium on Haptic Interfaces for Virtual Environment and Teleoperator Systems*. IEEE, Reno, NV, USA, 477–478. https://doi.org/10.1109/HAPTICS.2008.4479998

[44] Tomoya Sasaki, Richard Sahala Hartanto, Kao-Hua Liu, Keitarou Tsuchiya, Atsushi Hiyama, and Masahiko Inami. 2018. Leviopole: mid-air haptic interactions using multirotor. In *ACM SIGGRAPH 2018 Emerging Technologies* (Vancouver, British Columbia, Canada) *(SIGGRAPH '18)*. Association for Computing Machinery, New York, NY, USA, Article 12, 2 pages. https://doi.org/10.1145/3214907.3214913

[45] Tomoya Sasaki, Kao-Hua Liu, Taiki Hasegawa, Atsushi Hiyama, and Masahiko Inami. 2019. Virtual Super-Leaping: Immersive Extreme Jumping in VR. In *Proceedings of the 10th Augmented Human International Conference 2019* (Reims, France) *(AH2019)*. Association for Computing Machinery, New York, NY, USA, Article 18, 8 pages. https://doi.org/10.1145/3311823.3311861

[46] Shuntaro Shimizu, Takeru Hashimoto, Shigeo Yoshida, Reo Matsumura, Takuji Narumi, and Hideaki Kuzuoka. 2021. Unident: Providing Impact Sensations on Handheld Objects via High-Speed Change of the Rotational Inertia. In *2021 IEEE Virtual Reality and 3D User Interfaces (VR)*. IEEE, Lisbon, Portugal, 11–20. https://doi.org/10.1109/VR50410.2021.00021

[47] Misha Sra, Abhinandan Jain, and Pattie Maes. 2019. Adding Proprioceptive Feedback to Virtual Reality Experiences Using Galvanic Vestibular Stimulation. In *Proceedings of the 2019 CHI Conference on Human Factors in Computing Systems* (Glasgow, Scotland Uk) *(CHI '19)*. Association for Computing Machinery, New York, NY, USA, 1–14. https://doi.org/10.1145/3290605.3300905

[48] Fritz Strack. 1992. Order effects in survey research: Activation and information functions of preceding questions. In *Context effects in social and psychological research*, Norbert Schwarz and Seymour Sudman (Eds.). Springer, New York, NY, USA, 23–34.

[49] Yuning Su, Weizhi Nai, Xiaoying Sun, and Zuowei Sun. 2021. Design and Modeling of an Ungrounded Haptic Gun that Simulates Recoil Using Asymmetric Force. In *2021 IEEE World Haptics Conference (WHC)*. IEEE, Montreal, QC, Canada, 361–366. https://doi.org/10.1109/WHC49131.2021.9517202

[50] Fong Wee Teck, Huang Zhiyong, Farzam Farbiz, Cher Jingting, Chin Ching Ling, and Susanto Rahardja. 2011. Ungrounded handheld device for simulating high-forces of ball impacts in virtual tennis. In *SIGGRAPH Asia 2011 Emerging Technologies*. ACM, Hong Kong, China, 1–1.

[51] Ching-Yi Tsai, I-Lun Tsai, Chao-Jung Lai, Derrek Chow, Lauren Wei, Lung-Pan Cheng, and Mike Y. Chen. 2022. AirRacket: Perceptual Design of Ungrounded, Directional Force Feedback to Improve Virtual Racket Sports Experiences. In *Proceedings of the 2022 CHI Conference on Human Factors in Computing Systems* (New Orleans, LA, USA) *(CHI '22)*. Association for Computing Machinery, New York, NY, USA, Article 185, 15 pages. https://doi.org/10.1145/3491102.3502034

[52] Hsin-Ruey Tsai and Bing-Yu Chen. 2019. ElastImpact: 2.5D Multilevel Instant Impact Using Elasticity on Head-Mounted Displays. In *Proceedings of the 32nd Annual ACM Symposium on User Interface Software and Technology* (New Orleans, LA, USA) *(UIST '19)*. Association for Computing Machinery, New York, NY, USA, 429–437. https://doi.org/10.1145/3332165.3347931

[53] Hsin-Ruey Tsai, Yu-So Liao, and Chieh Tsai. 2022. ImpactVest: Rendering Spatio-Temporal Multilevel Impact Force Feedback on Body in VR. In *Proceedings of the 2022 CHI Conference on Human Factors in Computing Systems* (New Orleans, LA, USA) *(CHI '22)*. Association for Computing Machinery, New York, NY, USA, Article 356, 11 pages. https://doi.org/10.1145/3491102.3501971

[54] Hsin-Ruey Tsai, Jun Rekimoto, and Bing-Yu Chen. 2019. ElasticVR: Providing Multilevel Continuously-Changing Resistive Force and Instant Impact Using

Elasticity for VR. In *Proceedings of the 2019 CHI Conference on Human Factors in Computing Systems* (Glasgow, Scotland Uk) *(CHI '19)*. Association for Computing Machinery, New York, NY, USA, 1–10. https://doi.org/10.1145/3290605.3300450

[55] Julie M. Walker, Michael Raitor, Alex Mallery, Heather Culbertson, Philipp Stolka, and Allison M. Okamura. 2016. A dual-flywheel ungrounded haptic feedback system provides single-axis moment pulses for clear direction signals. In *2016 IEEE Haptics Symposium (HAPTICS)*. IEEE, Philadelphia, PA, USA, 7–13. https://doi.org/10.1109/HAPTICS.2016.7463148

[56] Yu-Wei Wang, Yu-Hsin Lin, Pin-Sung Ku, Yōko Miyatake, Yi-Hsuan Mao, Po Yu Chen, Chun-Miao Tseng, and Mike Y. Chen. 2021. JetController: High-Speed Ungrounded 3-DoF Force Feedback Controllers Using Air Propulsion Jets. In *Proceedings of the 2021 CHI Conference on Human Factors in Computing Systems* (Yokohama, Japan) *(CHI '21)*. Association for Computing Machinery, New York, NY, USA, Article 124, 12 pages. https://doi.org/10.1145/3411764.3445549

[57] Kyle N. Winfree, Jamie Gewirtz, Thomas Mather, Jonathan Fiene, and Katherine J. Kuchenbecker. 2009. A high fidelity ungrounded torque feedback device: The iTorqU 2.0. In *World Haptics 2009 - Third Joint EuroHaptics conference and Symposium on Haptic Interfaces for Virtual Environment and Teleoperator Systems*. IEEE, Salt Lake City, UT, USA, 261–266. https://doi.org/10.1109/WHC.2009.4810866

[58] Kyle N. Winfree, Joseph M. Romano, Jamie Gewirtz, and Katherine J. Kuchenbecker. 2010. Control of a high fidelity ungrounded torque feedback device: The iTorqU 2.1. In *2010 IEEE International Conference on Robotics and Automation*. IEEE, Anchorage, Alaska, USA, 1347–1352. https://doi.org/10.1109/ROBOT.2010.5509485

[59] Bob G Witmer and Michael J Singer. 1998. Measuring presence in virtual environments: A presence questionnaire. *Presence* 7, 3 (1998), 225–240.

[60] Xing-Dong Yang, Walter F Bischof, and Pierre Boulanger. 2008. Perception of haptic force magnitude during hand movements. In *2008 IEEE International Conference on Robotics and Automation*. IEEE, IEEE, Pasadena, CA, USA, 2061–2066.

[61] H. Yano, M. Yoshie, and H. Iwata. 2003. Development of a non-grounded haptic interface using the gyro effect. In *11th Symposium on Haptic Interfaces for Virtual Environment and Teleoperator Systems, 2003. HAPTICS 2003. Proceedings*. IEEE, Los Angeles, CA, USA, 32–39. https://doi.org/10.1109/HAPTIC.2003.1191223

[62] Run Yu and Doug A. Bowman. 2020. Pseudo-Haptic Display of Mass and Mass Distribution During Object Rotation in Virtual Reality. *IEEE Transactions on Visualization and Computer Graphics* 26, 5 (2020), 2094–2103. https://doi.org/10.1109/TVCG.2020.2973056